Age-related differences in fMRI subsequent memory effects are directly linked to local grey matter volume differences

Jasmin M. Kizilirmak*[,1,2,3], Joram Soch[1,4], Anni Richter[5,6], Björn H. Schott[1,5,7]

1) Cognitive Geriatric Psychiatry Group, German Center for Neurodegenerative Diseases, Göttingen, Germany
2) Neurodidactics and NeuroLab, Institute for Psychology, University of Hildesheim, Hildesheim, Germany
3) German Centre for for Higher Education Research and Science Studies, Hannover, Germany
4) Bernstein Center for Computational Neuroscience, Berlin, Germany
5) Leibniz Institute for Neurobiology, Magdeburg, Germany
6) Center for Intervention and Research on adaptive and maladaptive brain Circuits underlying mental health (C-I-R-C), Jena-Magdeburg-Halle, Germany
7) Department of Psychiatry and Psychotherapy, University Medical Center Göttingen, Göttingen, Germany

*Correspondence shall be addressed to J.M.K, kizilirmak@uni-hildesheim.de, or B.H.S., bschott@lin-magdeburg.de / bjoern-hendrik.schott@dzne.de

Disclosure statement/conflicts of interest: The authors have nothing to disclose.

Data availability: The data and analysis scripts/toolboxes used here are available online and linked in the Methods section.

Abstract

Episodic memory performance declines with increasing age, and older adults typically show reduced activation of inferior temporo-parietal cortices in functional magnetic resonance imaging (fMRI) studies of episodic memory formation. Given the age-related cortical volume loss, it is likely that age-related reduction of memory-related fMRI activity can partially be attributed to reduced grey matter volume (GMV). We performed a voxel-wise multimodal neuroimaging analysis of fMRI correlates of successful memory encoding, using regional GMV as covariate. In a large cohort of healthy adults (106 young, 111 older), older adults showed reduced GMV across the entire neocortex and reduced encoding-related activation of inferior temporal and parieto-occipital cortices compared to young adults. Importantly, these reduced fMRI activations during successful encoding in older adults could in part be attributed to lower regional GMV. Our results highlight the importance of controlling for structural MRI differences in fMRI studies in older adults but also demonstrate that age-related differences in memory-related fMRI activity cannot be attributed to structural variability alone.

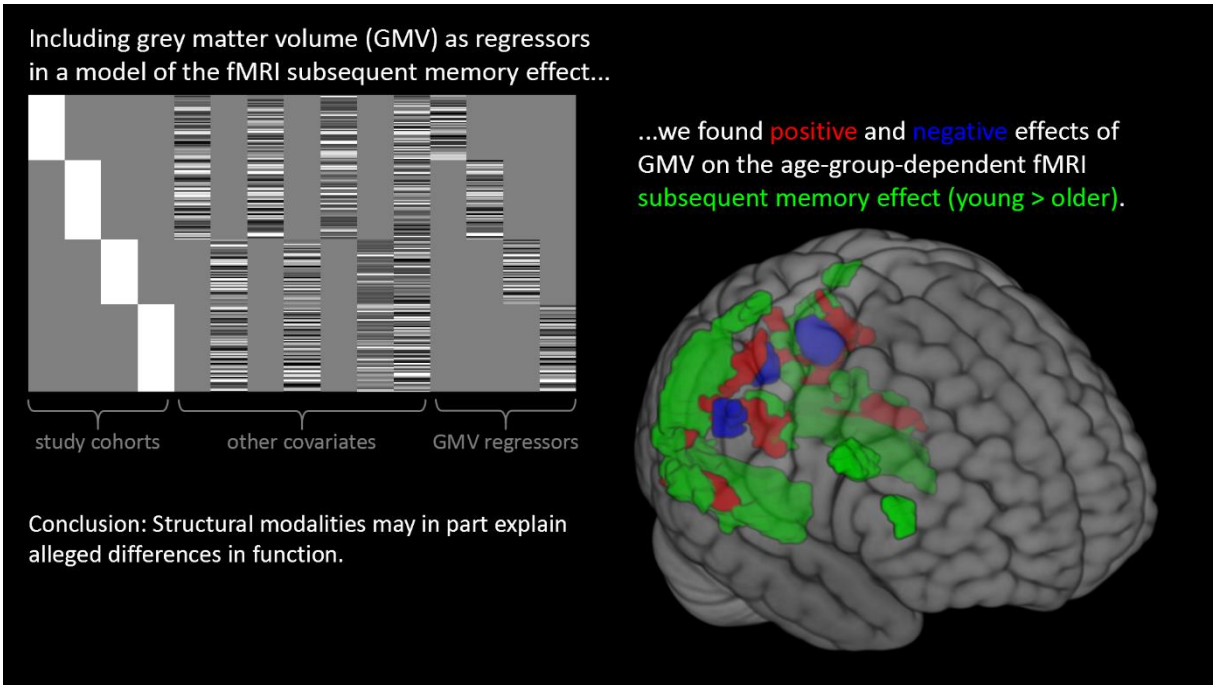

1. Introduction

Converging evidence supports an important link between cerebral and cognitive aging, especially with regard to episodic memory function (Cabeza et al., 2005; Nyberg et al., 2012). At an older age, considerable volume loss can be observed. White matter loss is associated with slower reaction times and neurocognitive processing in general, and grey matter loss is associated with a decline in cognitive performance, particularly in attention-demanding, working memory, and episodic memory tasks (Craik and Rose, 2012; Rönnlund et al., 2005). Most studies on the cognitive neuroscience of aging link structural and functional brain changes via behavioral performance measures (Persson et al., 2006; Soch et al., 2022), but only few have directly assessed the relationship between local structural and functional age-related differences with multimodal analyses (Boller et al., 2017; Kalpouzos et al., 2012). However, the latter is highly important to illuminate the relationship between brain maintenance on the one hand and cognitive reserve on the other. Direct conclusions on age-related differences in the functional recruitment of brain regions can only be drawn when considering potential links to local differences in brain structure.

Here, building on previous analyses of the same data set (Kizilirmak et al., 2022), we assessed the direct relationship between functional magnetic resonance imaging (fMRI) correlates of successful episodic memory encoding (subsequent memory effects, SME) and grey matter volume (GMV) in a large sample of young and older healthy adults using multimodal neuroimaging.

2. Material and methods

2.1. Participants

The sample consisted of 217 neurologically and psychiatrically healthy, right-handed adults who participated after having provided written informed consent. The 106 young participants (47 male, 59 female) had an age range of 18 to 35 years (mean age 24.12 ± 4.00 years). The 111 older participants (46 male, 65 female) had an age range of 60 to 80 years

(mean age 67.28 ± 4.65 years). A more detailed description of the study sample can be found in a previous paper by Soch and colleagues (Soch et al., 2021a, Table 1).

2.2. Stimuli, task, and procedure

The paradigm consisted of an encoding and a recognition session with a retention interval of approximately 60 min. Participants encoded 90 unique photographs of scenes incidentally, while performing an indoor/outdoor decision. 88 of the images were presented once during encoding, and two images were familiarized prior to the encoding phase and then repeated 22 times each during encoding, thus allowing for the construction of novelty contrasts (images presented once vs. repeatedly presented 'master' images). Recognition memory was tested in a surprise memory test, in which all 90 images from encoding plus 44 new images were presented. Participants provided recognition-confidence ratings on a 5-point rating scale ('sure new' over 'undecided' to 'sure old'). A more detailed description of the paradigm can be found in (Soch et al., 2021a).

2.3. MRI data acquisition

Structural and functional MRI data was acquired on two Siemens 3T MR scanners (Siemens Verio: 58 young, 64 older; Siemens Skyra: 48 young, 47 older). A T1-weighted magnetization-prepared rapid gradient echo (MPRAGE) image (TR = 2.5 s, TE = 4.37 ms, flip-α = 7°; 192 slices, 256 x 256 in-plane resolution, voxel size = 1 x 1 x 1 mm) was acquired for regional grey matter assessment via voxel-based morphometry (VBM) and for optimized normalization of fMRI data. Functional data comprised T2*-weighted echo-planar images (EPI; TR = 2.58 s, TE = 30 ms, flip-α = 80°; 47 axial slices, 64 x 64 in-plane resolution, voxel size = 3.5 x 3.5 x 3.5 mm) which were acquired while participants performed the encoding phase of the subsequent memory paradigm (8:51 min; 206 EPIs). Additionally, phase and magnitude fieldmap images were acquired to improve correction for artifacts resulting from magnetic field inhomogeneities. T2-weighted FLAIR images (192 sagittal slices, TR = 5.0 s, TE = 395 ms, 256 x 256 mm in-plane resolution, voxel size = 1.0 x 1.0 x 1.0 mm) were

acquired to assess white matter lesions.

2.4. MRI data analysis

VBM was used for the assessment of voxel-wise GMV and total intracranial volume (TIV), as implemented in the Computational Anatomy Toolbox (CAT12, http://www.neuro.uni-jena.de/cat/; Gaser & Dahnke, 2016), following a previously described protocol (Assmann et al., 2021; Richter et al., 2022). Segmented GM images were normalized to the Montreal Neurological Institute (MNI) reference frame, using the SPM12 DARTEL template, employing a Jacobian modulation, and keeping the spatial resolution 1 mm isotropic. Normalized GM maps were smoothed with a Gaussian kernel of 6 mm at FWHM.

The FLAIR images were used to assess white matter lesion volume (WMLV) via automatic segmentation using the Lesion Prediction Algorithm (Schmidt, 2017), as implemented in the Lesion Segmentation Toolbox (LST v3.0.0; https://www.applied-statistics.de/lst.html) based on CAT12 (see also Gaubert et al., 2023).

Preprocessing of fMRI data was carried out using Statistical Parametric Mapping, version 12 (SPM12; Wellcome Trust Center for Neuroimaging, University College London, UK; https://www.fil.ion.ucl.ac.uk/spm/). EPIs were corrected for acquisition time delay (*slice timing*), head motion (*realignment*) and magnetic field inhomogeneities (*unwarping*), using voxel-displacement maps derived from the fieldmaps. The MPRAGE image was spatially co-registered to the mean unwarped image and segmented into six tissue types, using the unified segmentation and normalization algorithm implemented in SPM12. The resulting forward deformation parameters were used to normalize unwarped EPIs into a standard stereotactic reference frame (MNI; voxel size = 3 x 3 x 3 mm). Normalized images were spatially smoothed using an isotropic Gaussian kernel of 6 mm full width at half maximum.

To assess the subsequent-memory effect from task fMRI, we specified a general linear model (GLM) for the fMRI data acquired during the encoding session. Two onset regressors for unique images (“novelty regressor”) and familiarized images (“master regressor”) were

created as box-car stimulus functions (2.5 s), convolved with the hemodynamic response function. The novelty regressor was parametrically modulated with the arcsine-transformed behavioral response rating from the recognition memory test, yielding a parametric subsequent memory regressor (Soch et al., 2021b). The model further included the six rigid-body movement parameters obtained from realignment as covariates of no interest, and a constant representing the implicit baseline. A positive effect of the parametric modulator reflects differential activation for remembered vs. forgotten items and is referred to as the subsequent memory effect.

2.5. Multi-modal MRI data analysis

The focus of the current study is on model 2 as reported in Kizilirmak et al. (2022). Multi-modal analyses were conducted using a toolbox[1] developed for use with SPM12. First-level fMRI contrast maps reflecting the parametric subsequent memory effect (SME) were used as the dependent variable, to be explained by two categorical factors *age group* (young, older) and *scanner* (1=Verio, 2=Skyra). The latter was included to account for potential effects of the different head coils. Continuous covariates of no interest to the current study were hippocampal volume, TIV and WMLV, separately modeled for each age group. Remaining variance within age groups was captured with an age regressor, mean-centered within age groups. Importantly, we further included one GMV regressor per each age group x scanner combination to add GMV as an explanatory variable. This way, we could specifically capture any effects of GMV in total and per age group on the fMRI subsequent memory effect. The design matrix is shown in Figure 1D. To provide an overview of the model:

SME ~ age group(young, old) + scanner(1, 2) + HC vol + TIV + WMLV + age + GMV.

All MATLAB scripts for the GLMs are provided at OSF[2] and the MRI data (GMV maps and SME contrast maps) at NeuroVault[3]. The significance level was set to $p < .05$, corrected

[1] https://github.com/JoramSoch/MMA
[2] https://osf.io/nzh2g/
[3] https://neurovault.org/collections/XDYPPLTD/

for family-wise error (FWE) at cluster level with a cluster-defining threshold of $p < .001$, uncorrected, and a minimum cluster size of 10 voxels.

3. Results

First, we assessed age-group differences in GMV and SME separately. As expected, there were pronounced differences in both cortical and subcortical GMV across the whole brain in the young > older contrast (Figure 1A), while few differences were found in the reverse contrast young < older, mainly along the border between GM and WM. As for the SME, and as reported previously (Kizilirmak et al., 2022, Figure 6; Soch et al., 2021a, Figure 2), the age differences in the SME included regions along the ventral and dorsal visual stream showing for young > older adults (Figure 1B) and mostly regions of the default mode network (DMN) for young < older adults, whereby the first differences are due to a higher activations in younger adults and the latter due to lower deactivations in the older adults.

Table 1. Positive and negative effects of GMV on the fMRI subsequent memory effect.

anatomical label	cluster size	cluster p(cFWE)	peak T	x.y.z {mm}
	positive effect			
	126	< .001	6.45	-30 -73 17
L middle occipital gyrus			5.99	-21 -61 32
			4.24	-18 -82 17
L middle temporal gyrus	104	< .001	6.30	-42 -55 -4
L lingual gyrus			4.50	-27 -67 -4
			4.50	-36 -70 -4
	122	< .001	5.89	27 -79 14
			4.87	21 -55 41
			4.83	30 -64 26
	69	< .001	5.62	39 -58 -7
R inferior occipital gyrus			4.94	36 -73 -7
R inferior temporal gyrus			4.40	45 -52 -7
	37	.017	5.08	24 -52 14
R precuneus			4.04	21 -46 8
	negative effect			
L precuneus	52	.003	6.95	-15 -61 32
R precuneus	33	.028	5.09	15 -58 32
R angular gyrus	36	.019	4.08	45 -46 29
			3.95	42 -46 20

Note. Reported are effects significant at $p < .05$ with FWE-correction at cluster level. A priori search threshold was set to $p < .001$, uncorrected, cluster size > 10 voxels.

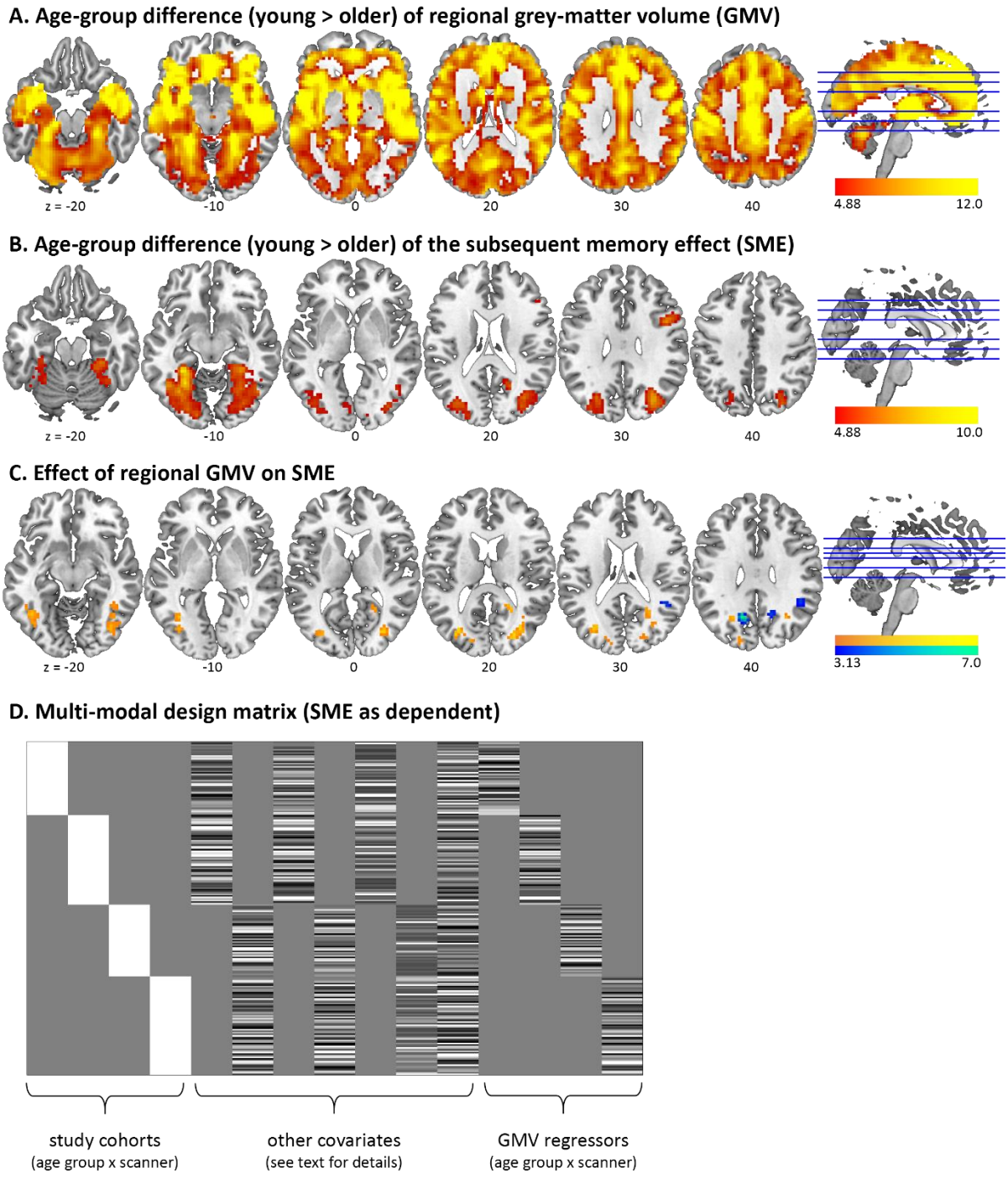

Figure 1. Effects of age differences in grey matter volume (GMV) and the fMRI subsequent memory effect (SME) as well as influences of GMV on SME. A. GMV contrast young > older. B. SME contrast young > older. C. Positive (warm colors) and negative (cold colors) effect of GMV on SME. D. Design matrix for the model used in B and C. Panels A and B show voxel-level FWE-corrected effects at p < .05, panels C and D show effects at cluster-defining threshold p < .001 uncorrected, all with a cluster threshold 10 voxels.

We then assessed the contribution of GMV to the observed SME (Table 1). While the main effect pattern remained qualitatively unchanged, our multi-modal analysis revealed positive as well as negative effects of GMV on SME (Figure 1C). Notably, the positive effects of GMV on SME (Table 1) were observed in overlapping occipital and lingual gyrus regions as the age effects on the SME itself (cf. Figure 1B vs. 1C).

4. Discussion

With the current study we directly assessed the relationship between local structural (GMV) and functional age-related differences during SME. To our knowledge, there has only been one study so far with this methodological approach (Kalpouzos et al., 2012). In 16 young (8 female) and 20 older healthy participants (all female), the authors investigated the influence of voxel-wise GMV on intentional episodic memory encoding. The authors masked the fMRI contrast maps with the thresholded encoding-versus-control contrast and looked at the main effect of GMV collapsed across age groups. They, too, reported that occipital GMV loss accounted for an underrecruitment during encoding, but could only infer this indirectly, as they were unable to differentiate positive and negative effects due to restrictions of the toolbox used (BPM, Casanova et al., 2007) In the present study, we followed up on this valuable multimodal approach using data from a much larger and more representational healthy population (106 young and 111 older adult, balanced gender distribution in both age groups), assessing both positive and negative effects of GMV on fMRI encoding contrasts. Further, fMRI activity related to successful encoding was assessed as a parametrically modelled SME for an incidental visual episodic encoding task that reflects later recognition, which is more specific than an encoding-versus-control contrast. Our results indicate that older adults showed reduced activations during successful encoding of visual scenes in the same regions in which they show significant reductions in GMV, that is, occipital and lingual gyrus, as well as middle temporal lobe. Moreover, we found a direct association between regional GMV and successful encoding-related fMRI. This demonstrates the importance of

taking structural differences into account when comparing fMRI effects in different age groups that these structural differences cannot be completely "compensated" by normalizing the data to standard brain templates like MNI. Notably, the GMV effects on the fMRI subsequent memory effect were in occipital brain regions despite the observation that GMV age differences were most pronounced frontally (Figure 1A). This can probably be explained by the fact that we used a visual memory encoding task, supporting modality dependence.

Another important finding was that age-related differences in fMRI subsequent memory effects are robust, even when individual regional GMV differences are accounted for (Figure 1B). This is assuring regarding the many studies on age differences in episodic memory formation but cannot by itself be generalized to other participant groups, stimulus modalities and fMRI contrasts. We therefore highly recommend including structural modalities into the models when comparing fMRI effects of participant groups with differences in brain structure to detect potential confounds that may in part explain alleged differences in function.

5. Acknowledgements

This study was supported by the State of Saxony-Anhalt and the European Union (Research Alliance “Autonomy in Old Age” to A.R. and B.H.S.) and by the Deutsche Forschungsgemeinschaft (SFB 1436, TP A05). We thank Hartmut Schütze for programming the experimental paradigm . We thank our Hannah Feldhoff, Larissa Fischer, Lea Knopf, Matthias Raschick, and Annika Schult for their help with participant recruitment and data collection. We further thank Kerstin Möhring, Katja Neumann, Ilona Wiedenhöft, and Claus Tempelmann for help with MRI scanning.

6. References

Assmann A, Richter A, Schütze H, Soch J, Barman A, et al. 2021. Neurocan genome-wide psychiatric risk variant affects explicit memory performance and hippocampal function in healthy humans. *Eur J Neurosci* **53**:3942–3959. doi:10.1111/ejn.14872

Boller B, Mellah S, Ducharme-Laliberté G, Belleville S. 2017. Relationships between years of education, regional grey matter volumes, and working memory-related brain activity in healthy older adults. *Brain Imaging Behav* **11**:304–317. doi:10.1007/s11682-016-9621-7

Cabeza R, Nyberg L, Park D. 2005. Cognitive neuroscience of aging. Linking cognitive and cerebral aging., Cognitive Neuroscience of Aging: Linking cognitive and cerebral aging. Oxford, UK: Oxford University Press.

Casanova R, Srikanth R, Baer A, Laurienti PJ, Burdette JH, et al. 2007. Biological parametric mapping: A statistical toolbox for multimodality brain image analysis. *Neuroimage* **34**:137–143. doi:10.1016/j.neuroimage.2006.09.011

Craik FIM, Rose NS. 2012. Memory encoding and aging: A neurocognitive perspective. *Neurosci Biobehav Rev* **36**:1729–1739. doi:10.1016/j.neubiorev.2011.11.007

Gaser C, Dahnke R. 2016. CAT - A Computational Anatomy Toolbox for the Analysis of Structural MRI DataAnnual Meeting of the Organization of Human Brain Mapping.

Gaubert M, Dell'Orco A, Lange C, Garnier-Crussard A, Zimmermann I, et al. 2023. Performance evaluation of automated white matter hyperintensity segmentation algorithms in a multicenter cohort on cognitive impairment and dementia. *Front Psychiatry* **13**:1–14. doi:10.3389/fpsyt.2022.1010273

Kalpouzos G, Persson J, Nyberg L. 2012. Local brain atrophy accounts for functional activity differences in normal aging. *Neurobiol Aging* **33**:623.e1-623.e13. doi:10.1016/j.neurobiolaging.2011.02.021

Kizilirmak JM, Soch J, Schütze H, Düzel E, Feldhoff H, et al. 2022. The relationship between resting-state amplitude fluctuations and memory-related deactivations of the Default Mode Network in young and older adults. *PsyArXiv* 1–35. doi:10.31234/osf.io/vuym5

Nyberg L, Lövdén M, Riklund K, Lindenberger U, Bäckman L. 2012. Memory aging and brain maintenance. *Trends Cogn Sci* **16**:292–305. doi:10.1016/j.tics.2012.04.005

Persson J, Nyberg L, Lind J, Larsson A, Nilsson LG, Ingvar M, Buckner RL. 2006. Structure-function correlates of cognitive decline in aging. *Cereb Cortex* **16**:907–915.

doi:10.1093/cercor/bhj036

Richter A, Soch J, Kizilirmak JM, Fischer L, Schütze H, et al. 2022. Summary statistics of memory-related fMRI activity reflect dissociable neuropsychological and anatomical signatures of neurocognitive aging. *bioRxiv*. doi:10.1101/2022.02.04.479169

Rönnlund M, Nyberg L, Bäckman L, Nilsson LG. 2005. Stability, growth, and decline in adult life span development of declarative memory: Cross-sectional and longitudinal data from a population-based study. *Psychol Aging* **20**:3–18. doi:10.1037/0882-7974.20.1.3

Schmidt P. 2017. Bayesian inference for structured additive regression models for large-scale problems with applications to medical imaging. Ludwig- Maximilians-Universität München.

Soch J, Richter A, Kizilirmak JM, Schütze H, Feldhoff H, et al. 2022. Structural and Functional MRI Data Differentially Predict Chronological Age and Behavioral Memory Performance. *Eneuro* **9**:ENEURO.0212-22.2022. doi:10.1523/eneuro.0212-22.2022

Soch J, Richter A, Schütze H, Kizilirmak JM, Assmann A, et al. 2021a. A comprehensive score reflecting memory-related fMRI activations and deactivations as potential biomarker for neurocognitive aging. *Hum Brain Mapp* **42**:4478–4496. doi:10.1002/hbm.25559

Soch J, Richter A, Schütze H, Kizilirmak JM, Assmann A, et al. 2021b. Bayesian model selection favors parametric over categorical fMRI subsequent memory models in young and older adults. *Neuroimage* **230**:117820. doi:10.1016/j.neuroimage.2021.117820